Robotica (2004) volume 22, pp. 285–300. © 2004 Cambridge University Press
DOI: 10.1017/S0263574703005587 Printed in the United Kingdom

Modeling and simulation of planar flexible link manipulators with rigid tip connections to revolute joints

S. M. Megahed and K. T. Hamza

Faculty of Engineering, Cairo University, Giza 12316 (Egypt). E-Mail: smegahed@yahoo.com & kthamza@yahoo.com

(Received in Final Form: September 11, 2003)

SUMMARY

This paper presents the basis of a mathematical model for simulation of planar flexible-link manipulators, taking into consideration the effect of higher stiffness zones at the link tips. The proposed formulation is a variation of the finite segment multi-body dynamics approach. The formulation employs a consistent mass matrix in order to provide better approximation than the traditional lumped masses often encountered in the finite segment approach. The formulation is implemented into a computational code and tested through three examples; cantilever beam, rotating beam and three-link manipulator. In these examples, the length of the rigid tips at both sides of each link ranges from 0% to 6.25% of the whole link length. The zones of higher stiffness at the link tips are treated as short rigid zones. The effect of the rigid zones is averaged along with some portions of the flexible links, thereby allowing further simplification of the dynamic equations of motion. The simulation results demonstrate the effectiveness of the proposed modeling technique and show the importance of not ignoring the effect of the rigid tips.

KEYWORDS: Flexible manipulators modeling; Simulation algorithms; Multi-body dynamics.

1. INTRODUCTION

Flexible manipulators are well known for their advantages over rigid ones in having higher load to weight ratio, higher speeds and lower power consumption. The control schemes for flexible manipulators, which often present a challenge in order to obtain good performance out of them have thus become the target of extensive research.[1–9] Having a good tool for performance simulation is very useful in the development of flexible manipulator controllers. However, accurate simulation of flexible manipulators is not an easy task since the dynamic equations of motion are highly nonlinear and are often coupled. Furthermore, there is seldom an analytical solution for such systems except in very limited special cases.[10,11] Making use of Flexible Multi-body Dynamics techniques is a promising approach in simulation of flexible manipulators.[12–14] The most popular of those techniques are the Floating Frame of Reference,[15–17] Incremental Finite Element,[15] Absolute Nodal Coordinate,[15,16,18] Large Rotation Vector[15] and the Finite Segment approach.[15,19–22]

In this paper, the mathematical formulation presented in references [20,21] is modified to take into account the effect of the short rigid parts at the beginning and end of each link at the connections to joints (Figure 1). The proposed model is used for simulating many examples[22]. Three of these examples are presented in this paper: Cantilever beam, Rotating beam and a Three-link manipulator. The results of the frst two examples are compared with those obtained by conventional formulations. The simulation results show that ignoring the effect of the rigid tips may lead to incorrect results. The studied examples also demonstrate the effectiveness of the proposed technique in achieving results close to the conventional ones through simpler programming methodology. The third example is not compared with conventional solutions, but is included as a demonstration of the capability of the proposed formulation to simulate multi-link manipulators.

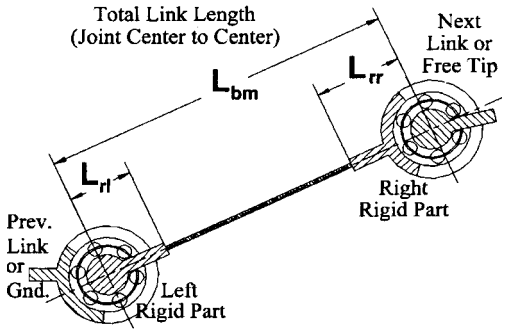

Fig. 1. An actual flexible manipulator link.

2. MATHEMATICAL MODELING

A variation of the Finite Segment approach is used to formulate the dynamic equations of motion. The finite segment approach generally assumes a flexible body to be composed of a number of discrete rigid segments that are connected by springs and/or dampers. This makes the treatment of a flexible link similar to the treatment of several rigid bodies. Each link is broken into elements connected at nodes (Figure 2). Revolute joints can be modeled as perfect joints (Figure 3-a) which have no internal clearance and are of infinite radial stiffness, or as flexible joints (Figure 3-b) that permit relative radial motion between the end of one link and the beginning of the next one. At any time instant, the relative positions, orientations and velocities can be used to compute the total stiffness and damping forces acting at each node. Then, by applying the principles of rigid body dynamics on each node the equations of motion are:

$$[M]\,[\ddot{x}] = [F] \tag{1}$$

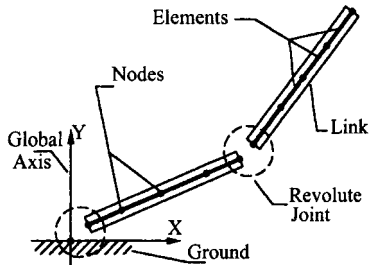

Fig. 2. Flexible manipulator model.

where $[F]$ is the total force vector representing the effect of the forces due to stiffness, damping, actuators and external loads, $[\dot{x}]$ is the nodal acceleration vector and $[M]$ is the manipulator mass matrix.

The generalized coordinates (Figure 4) are the global position (x_i, y_i) and the angular orientation θ_i of the i^{th} node in the system. In the case of single open chain manipulators, it is convenient to calculate the stiffness and damping forces directly rather than first assemble the stiffness and damping matrices and then multiply them by the deflections and velocities respectively.

External loads and actuating torques are added to the total force vector (Equation (1)) at the nodes upon which they act. It should be noted that it is possible to simulate the effect of a perfect actuator or to take the internal dynamics of the actuator into account. The torque induced at any instant by a perfect actuator acts on both links: the link on which it is mounted (connected to its stator) and the one it drives (connected to its rotor) by equal and opposite torque values.[23] On the other hand, an imperfect actuator can have different torque values upon the two connected links due to the effect of internal inertia, linear and nonlinear stiffness and damping in the power transmission system. Simulation of the effect of an imperfect actuator requires prior identification of its characteristics and is beyond the scope of the case studies provided in this paper.

Motion of the system is simulated by applying a numerical time-step integration technique on Equation (1). For that purpose, a fourth order Runge-Kutta[24] was used in all simulations presented in this paper.

2.1. *Element mass matrix*

In conventional Finite Segment approach, the mass matrix would be a diagonal matrix whose elements are the equivalent lumped masses at the nodes. Lumping ignores the inertia coupling between the nodes. Inertia coupling is characteristic of continuous systems.[16] So, ignoring it often results in lower accuracy of simulation even when a relatively large number of elements per link are being used.[20] Inertia coupling is introduced to the system of equations by assembling the element mass matrices obtained from consistent mass formulation of a two-node beam element.[25]

$$[m] = [R]^T [m]_e [R] \tag{2}$$

$$[m]_e = \rho L_{eo} \begin{bmatrix} \frac{1}{3} & 0 & 0 & \frac{1}{6} & 0 & 0 \\ 0 & \frac{13}{35} & \frac{11L_{eo}}{210} & 0 & \frac{9}{70} & \frac{-13L_{eo}}{420} \\ 0 & \frac{11L_{eo}}{210} & \frac{L_{eo}^2}{105} & 0 & \frac{13L_{eo}}{420} & \frac{-L_{eo}^2}{140} \\ \frac{1}{6} & 0 & 0 & \frac{1}{3} & 0 & 0 \\ 0 & \frac{9}{70} & \frac{13L_{eo}}{420} & 0 & \frac{13}{35} & \frac{-11L_{eo}}{210} \\ 0 & \frac{-13L_{eo}}{420} & \frac{-L_{eo}^2}{140} & 0 & \frac{-11L_{eo}}{210} & \frac{L_{eo}^2}{105} \end{bmatrix} \tag{3}$$

$$[R] = \begin{bmatrix} c_i & s_i & 0 & 0 & 0 & 0 \\ -s_i & c_i & 0 & 0 & 0 & 0 \\ 0 & 0 & 1 & 0 & 0 & 0 \\ 0 & 0 & 0 & c_i & s_i & 0 \\ 0 & 0 & 0 & -s_i & c_i & 0 \\ 0 & 0 & 0 & 0 & 0 & 1 \end{bmatrix} \tag{4}$$

where $[m]$ is the element mass matrix, $[R]$ is the rotation matrix, ρ is the mass per unit length of the beam, L_{eo} is the element length, $c_i = \cos(\theta_i)$ and $s_i = \sin(\theta_i)$.

The mass matrix in Equation (3) is obtained by ignoring the centrifugal and Coriollis acceleration terms, which allows treatment of a flexible link instantaneously as a structural member. Hence, it is possible to calculate the

Fig. 3. (a) A perfect revolute joint. (b) A flexbile revolute joint.

https://doi.org/10.1017/S0263574703005587 Published online by Cambridge University Press

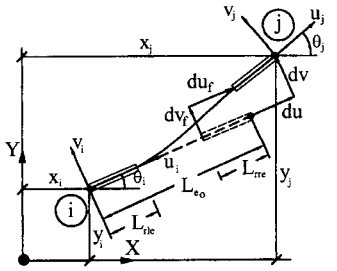

Fig. 4. An element in a general configuration.

mass matrix using the beam-element shape functions given in reference [25]:

$$N_1 = 1 - \zeta,\ N_2 = 3(1-\zeta)^2 - 2(1-\zeta)^3,\ N_3 = \zeta L_{eo}(1-\zeta)^2$$

$$N_4 = \zeta,\ N_5 = 3\zeta^2 - 2\zeta^3,\ N_6 = -L_{eo}(1-\zeta)\zeta^2 \tag{5}$$

Where ζ is the fraction of the length of the beam, starting from the first node.

It should be noted that although the centrifugal and Coriollis inertia terms are ignored in this formulation, their effect is generally minimal and decreases by increasing the number of segments in the flexible link model.

2.2. *Element stiffness forces*

An element in a general configuration is shown in Figure 4. The special formulation presented in this paper allows each element in the mesh to have rigid parts at its right and left ends. It is worth noting that in practical use of this formulation in simulation purposes (where a link is meshed using several elements), an element would either have its left end with a rigid part (first element), right end with a rigid part (last element) or no rigid parts at all (other elements). The formulation presented allows having a two rigid ends in the same element for the sake of generality. Thus, the same formulation of the element can be used in all cases by setting the length of the left rigid part (L_{rle}) or right rigid part (L_{rre}) to zero in case of their absence.

Employing simple trigonometric manipulations (see Figure 4), deflection of the flexible part of the element from its undeformed shape in the direction of the local element axes u_i and v_i is given by:

$$\begin{bmatrix} du_f \\ dv_f \end{bmatrix} = \begin{bmatrix} c_i & s_i \\ -s_i & c_i \end{bmatrix} \begin{bmatrix} x_j - x_i - L_{rre}(c_j - c_i) \\ y_j - y_i - L_{rre}(s_j - s_i) \end{bmatrix} - \begin{bmatrix} L_{eo} \\ 0 \end{bmatrix}$$

$$d\theta_f = \theta_j - \theta_i \tag{6}$$

The deflections are used to compute the stiffness forces in the direction of element axis as well as the stiffness moment. The stiffness forces are then transformed to the direction of the global axes in order to be assembled in the total force vector (Equation (1)). The stiffness forces and moment are given by:

$$F_{kui} = K_a du_f$$

$$F_{kvi} = K_{b1} dv_f - K_{b2} d\theta_f$$

$$M_{kzi} = -K_{b2} dv_f + K_{b3} d\theta_f - F_{kvi} L_{rre}$$

$$M_{kzj} = -M_{kzi} - F_{kvi}(L_{eo} - L_{rre}) \tag{7}$$

$$\begin{bmatrix} F_{kxi} \\ F_{kyi} \end{bmatrix} = \begin{bmatrix} c_i & -s_i \\ s_i & c_i \end{bmatrix} \begin{bmatrix} F_{kui} \\ F_{kvi} \end{bmatrix} \ \&\ \begin{bmatrix} F_{kxj} \\ F_{kyj} \end{bmatrix} = \begin{bmatrix} -F_{kxi} \\ -F_{kyi} \end{bmatrix} \tag{8}$$

Where the stiffness constants of the element are given by:

$$K_a = \frac{E_e A_e}{L_f},\ K_{b1} = \frac{12 E_e I_e}{L_f^3},\ K_{b2} = \frac{6 E_e I_e}{L_f^2},\ K_{b3} = \frac{4 E_e I_e}{L_f}$$

$$\&\ L_f = (L_{eo} - L_{rle} - L_{rre}) \tag{9}$$

where E_e is the beam modulus of elasticity, A_e is its cross sectional area, I_e is its second moment of area and L_f is the length of the flexible part of the element.

It should be noted that this manner of computing the stiffness forces is analogous to multiplying the stiffness matrix by the deflection vector in beam elements formulated in traditional finite element.[25] Thus, using the proposed model in simulation will give almost exactly the same results when simulating structural dynamics problems. However, in traditional finite element, rigid body rotation of the beam element does not result in zero strain, which limits the use of the traditional beam element in solving problems involving large rotations.[15] Equation (7) however, permits rigid body rotation with zero strain because element deflections are calculated as the relative position of the nodes with respect to the undeformed shape (Figure 4).

2.3. *Element damping forces*

Several traditional methods are used to express the damping effect of structural members.[25–28] One of the most popular methods is known as Rayleigh damping, in which, an equivalent viscous damping matrix is defined as a linear combination of the mass and stiffness matrices. In this case, the element damping forces[26] will be:

$$[F]_c = [C][\dot{x}] = [F]_{cm} + [F]_{ck}$$

$$[F]_{cm} = \alpha[m]\ \&\ [F]_{ck} = \beta[k] \tag{10}$$

where $[F]_c$ is the element damping force vector, $[F]_{cm}$ and $[F]_{ck}$ are the mass and stiffness associated damping forces respectively, $[\dot{x}]$ is the nodal velocity vector, $[C]$, $[m]$ and $[k]$ are the element damping, mass and stiffness matrices respectively. α and β are the element damping constants. These damping constants are not readily known as the stiffness constants, experimental identification of them is recommended for better accuracy of simulation.[21]

https://doi.org/10.1017/S0263574703005587 Published online by Cambridge University Press

Table I. Beam Data of Examples #1 and #2.

Link length (L_{bm})	0.8 m
Length of Left Rigid Zone	0.00 to 0.05 m step 0.01 m
Length of Right Rigid Zone	0.00 to 0.05 m step 0.01 m
Modulus of Elasticity × Cross Sectional Area (E_eA_e)	1.8×10 N
Modulus of Elasticity × Second Moment of Area (E_eI_e)	13.5 N.m^2
Mass Associated Damping Constant (α)	0.1 (SI units)
Stiffness Associated Damping Constant (β)	1.6×10^{-4} (SI units)
Mass per unit length	0.72 kg/m
Number of Elements per link	4
Plane of motion	Horizontal Plane
Loading	Unit Step Force at Free Tip
Simulation time	0.5 s

In the proposed formulation, the term $[F]_{cm}$ is the same as in Rayleigh damping. $[F]_{ck}$ is to be calculated in a similar manner as the stiffness forces through computing the relative velocity between the nodes of the element in the direction of the element axes then computing the stiffness associated damping forces similar to Equation (8). The relative velocities between the nodes are given by:

$$\begin{bmatrix} d\dot{u}_f \\ d\dot{v}_f \end{bmatrix} = \begin{bmatrix} c_i & s_i \\ -s_i & c_i \end{bmatrix} \begin{bmatrix} \dot{x}_j - \dot{x}_i + L_{rre}(s_j\dot{\theta}_j - s_i\dot{\theta}_i) \\ \dot{y}_j - \dot{y}_i - L_{rre}(c_j\dot{\theta}_j - c_i\dot{\theta}_i) \end{bmatrix}$$

$$- \dot{\theta}_i \begin{bmatrix} s_i & -c_i \\ c_i & s_i \end{bmatrix} \begin{bmatrix} x_j - x_i - L_{rre}(c_j - c_i) \\ y_j - y_i - L_{rre}(s_j - s_i) \end{bmatrix}$$

$$d\dot{\theta}_f = \dot{\theta}_j - \dot{\theta}_i \tag{11}$$

The damping forces and damping constants are given by:

$$\begin{aligned} F_{cui} &= C_a d\dot{u}_f \\ F_{cvi} &= C_{b1} d\dot{v}_f - C_{b2} d\dot{\theta}_f \\ M_{czi} &= -C_{b2} d\dot{v}_f + C_{b3} d\dot{\theta}_f - F_{cvi} L_{rre} \\ M_{czj} &= -M_{czi} - F_{cvi}(L_{eo} - L_{rre}) \end{aligned} \tag{12}$$

$$\begin{bmatrix} F_{cxi} \\ F_{cyi} \end{bmatrix} = \begin{bmatrix} c_i & -s_i \\ s_i & c_i \end{bmatrix} \begin{bmatrix} F_{cui} \\ F_{cvi} \end{bmatrix} \;\&\; \begin{bmatrix} F_{cxj} \\ F_{cyj} \end{bmatrix} = \begin{bmatrix} -F_{cxi} \\ -F_{cyi} \end{bmatrix} \tag{13}$$

$$C_a = \beta K_a,\ C_{b1} = \beta K_{b1},\ C_{b2} = \beta K_{b2} \;\&\; C_{b3} = \beta K_{b3} \tag{14}$$

It should be noted that Equation (11) is the generalized form of the similar equation given in references [20, 21].

3. APPLICATION EXAMPLES

The following examples are intended to assess the effectiveness of the proposed formulation in simulating the motion of flexible links that have rigid parts at their tips. The values of the damping constants used in the examples are chosen close to the values obtained in reference [21]. For more accurate simulation of the true link behavior, experimentally identified values of these constants should be performed. The objective of these examples, however, is to compare results using the proposed formulation and the conventional one rather than performing a simulation of the true link behavior.

3.1. Example #1: Vibrating cantilever beam

In order to assess the effectiveness of the proposed formulation in simulating the motion of flexible manipulators, first the transient state vibrations of a flexible cantilever beam that has rigid parts at its beginning and free tip due to a step force at the free tip is studied (Figure 5-a). The beam data is given in Table I.

The conventional solution, which is taken as a reference involves meshing only the flexible part of the beam (Figure 5-b). The force at the tip is transformed to the end-node in addition to a moment. Inertia forces due to the mass of the rigid part at the free tip are also added at the end-node.

The essential difference in using the proposed formulation presented in this paper is that the whole length of the beam is meshed (Figure 5-c). The first and last elements thus contain a rigid part (Figure 6) and are thus of higher stiffness than the rest of the elements in the mesh. The proposed formulation ensures that the stiffness and stiffness associated damping forces are equivalent to those resulting from the conventional method. However, the mass matrix of the element is slightly different since the deflection line of the rigid-flexible parts is slightly different from the approximated deflection line of the element in the proposed formulation. This slight difference causes a small error in the simulation using the proposed formulation (about 4% in

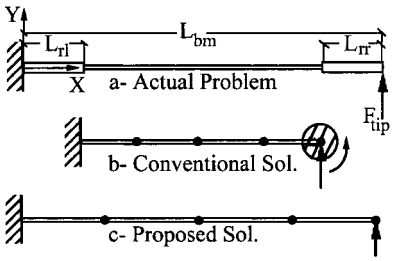

Fig. 5. A flexible cantilever beam with rigid tips.

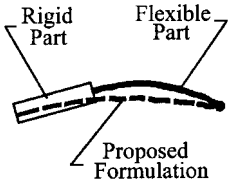

Fig. 6. Approximation of a rigid and a flexible part in one element.

https://doi.org/10.1017/S0263574703005587 Published online by Cambridge University Press

the presented examples). This error is further reduced when the stiffness of the element is higher and thus the deflection is lower as will be demonstrated. Despite this error, the system dynamic equations are vastly simplified in them since there is no need to add extra inertia forces as in the conventional solution and more importantly, the constraint equations of a revolute joint become far simpler as will be demonstrated in the second example.

Results of conventional formulation: The transient response of the beam for different values of the ength of the rigid parts (0.0%, 1.25%, 2.5%, 3.75%, 5.0% and 6.25%) is obtained using 4 elements per link mesh (Figure 7). A check to confirm that 4 elements per link gives sufficient simulation accuracy is performed by carrying out a comparison with the solution obtained using 8 elements per link. The two solutions are so closely matching that plotting them on the same graph would reveal little. Instead, the difference between the two solutions is given in Figure 8. It is shown that the solution difference between 4 and 8 elements per link is pretty small, thus the solution using 4 elements per link is sufficiently accurate to be taken as a reference. It is shown by Figure 7 that the response of the no-rigid part beam (0.0%) can be pretty different than if the beam contains rigid parts. Thus, ignoring the effect of the rigid parts may lead to completely inaccurate simulation results.

Results of proposed formulation: The solution obtained using 4 elements per link is shown in Figure 9. The difference between the proposed and conventional solutions is given in Figures 10 and 11. Figure 10 shows the effect of the ratio of the length of rigid part to that of the overall length of the beam (solution obtained using 4 elements per link). Figure 11 shows the effect of the ratio of length of the rigid part to the length of the element in the proposed mesh (solution obtained for $L_{rl}/L_{bm}=L_{rr}/L_{bm}=6.25\%$ using 4, 6 & 8 elements per link).

3.2. Example #2: Rotating flexible beam

Since it sometimes happens that a certain formulation of a problem works well in some special cases but not so well in others, the performance of the proposed formulation is also tested on a rotating flexible arm (Figure 12). The beam properties are the same as in the previous case study and are given in Table I. Initial conditions are zero initial strain and velocity with the manipulator arm aligned with the X-axis (θ is zero at all nodes). No forces or movement act at the free tip, and a driving torque T_{hub} given by Figure 13 acts upon the hub. The revolute joint is assumed perfect.

Equivalent rigid system: It is also useful for the sake of motion trend evaluation, to know the response of the equivalent rigid body system. In the presence of damping, Equation (10), which expresses the damping forces and moments, is reduced and added to system equation of motion of the rigid system. The equation of motion becomes:

$$J\ddot{\theta}=T_{hub}-\alpha J\dot{\theta} \tag{15}$$

where J is the polar moment of inertia about the joint. The response of the rigid system both in the presence and absence of damping is given in Figure 14.

Results of conventional formulation: The conventional solution is achieved by using the same element mesh as in

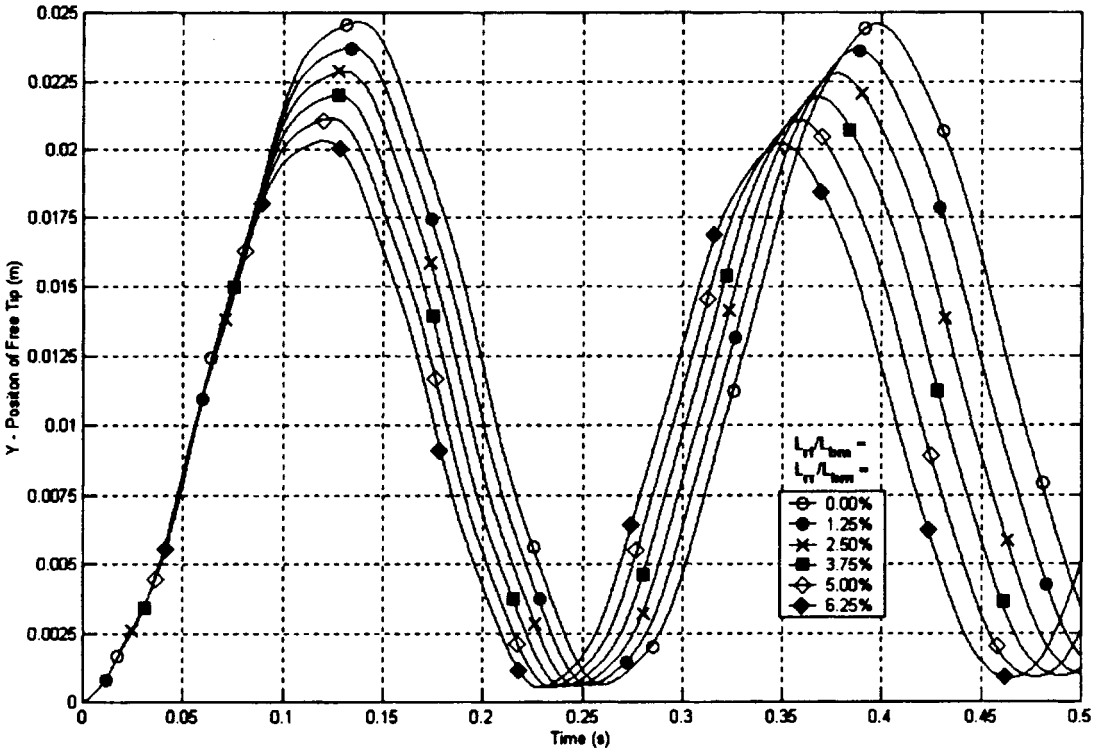

Fig. 7. Beam transient response – conventional formulation.

https://doi.org/10.1017/S0263574703005587 Published online by Cambridge University Press

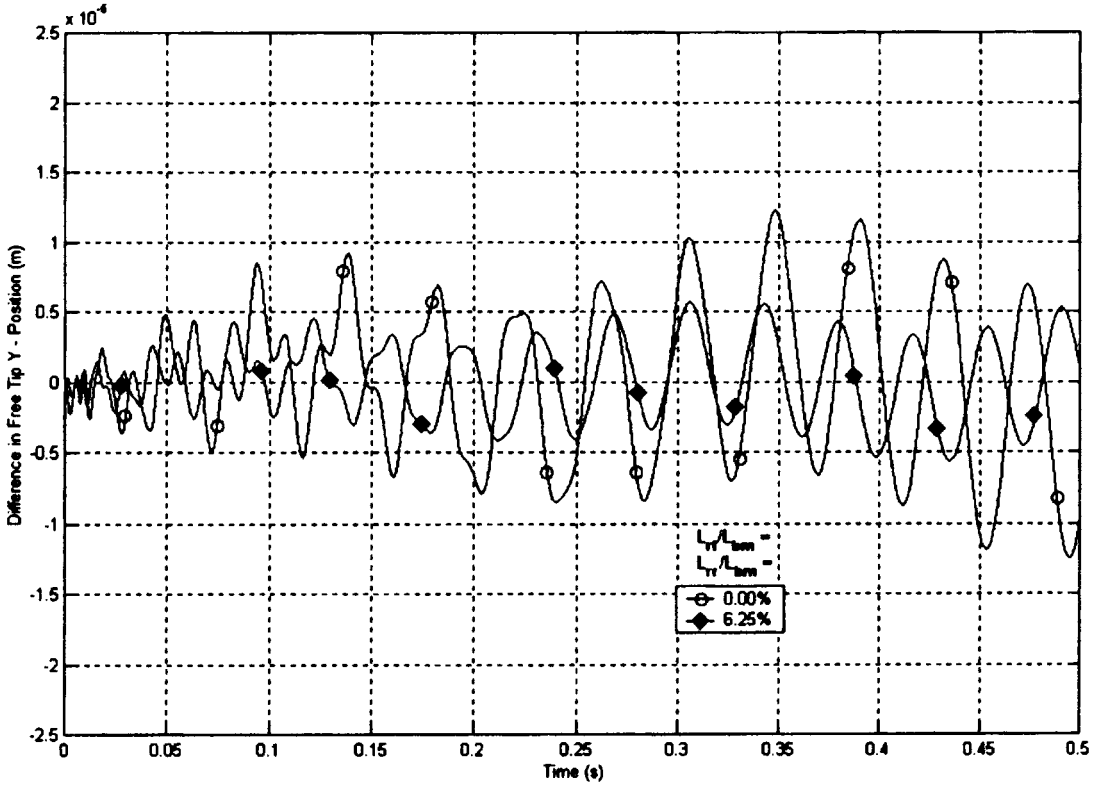

Fig. 8. Difference in simulation using 4 and 8 elements.

the previous case study. The constraint equations on node #1 due to the presence of the revolute joint are:

$$x_1 = L_{rl}\cos(\theta_1)$$
$$y_1 = L_{rl}\sin(\theta_1) \tag{16}$$

The constraint equations represented by Equation (14) are nonlinear algebraic equations. The process of solving a system containing both differential and algebraic equations involves differentiating the algebraic equations and using them to reduce the number of differential equations. A numeric technique for this purpose is presented in reference

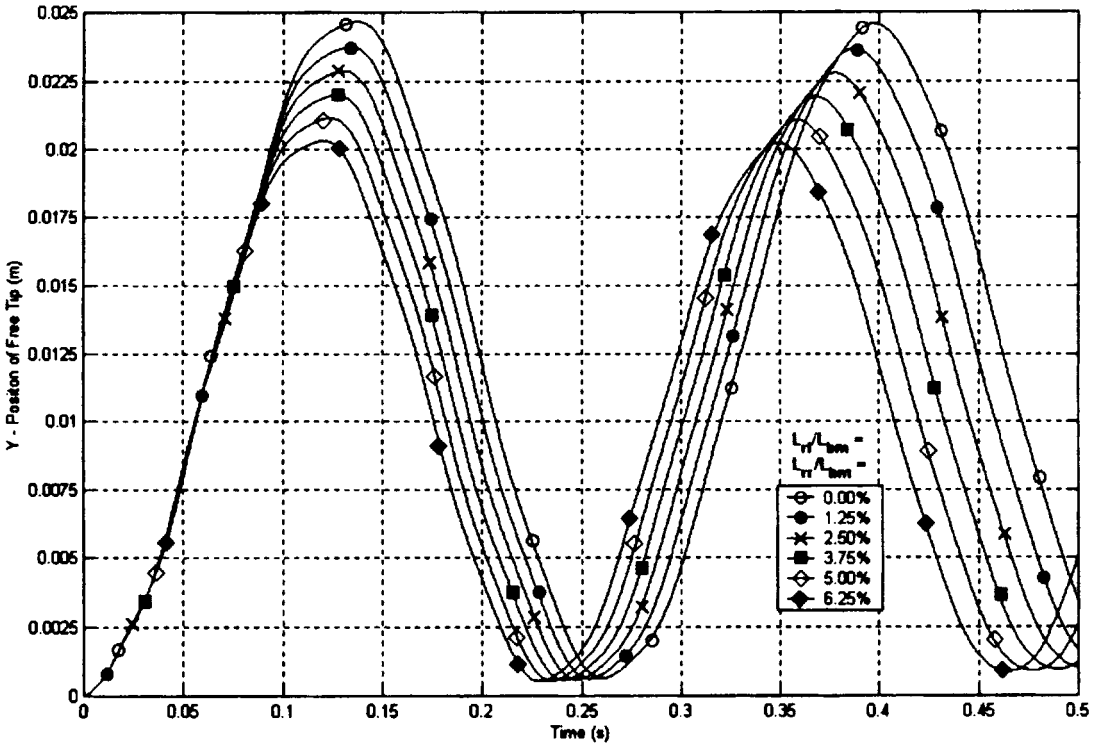

Fig. 9. Beam transient response – proposed formulation.

https://doi.org/10.1017/S0263574703005587 Published online by Cambridge University Press

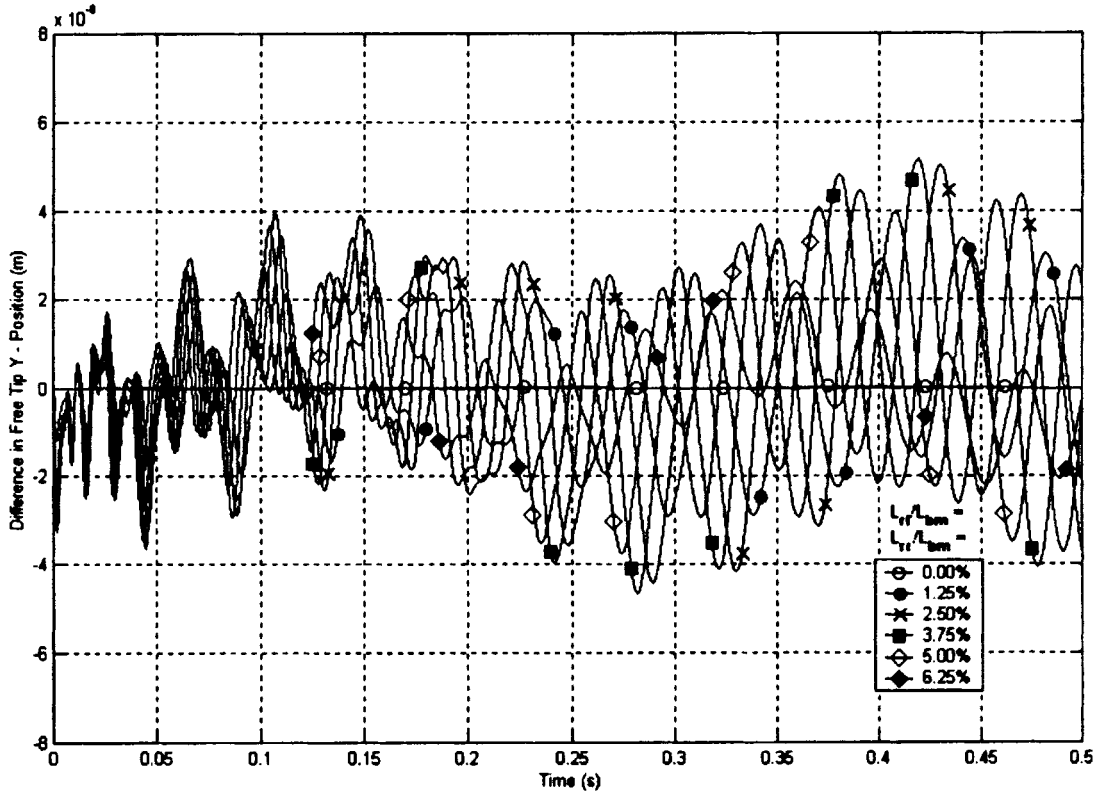

Fig. 10. Effect of rigid part w.r.t beam length.

[29], the equation reduction in this example however, was symbolically accomplished.

The conventional solution using 4 elements per link for different values of the ratio between the length of rigid part and the arm length shows only little differences, which can only be observed through magnification of parts of the time response (Figure 15). While this may be a justification for the approximation of ignoring the rigid tips, which is often done in the literature, this approximation is not applicable in all cases as demonstrated in the previous case study.

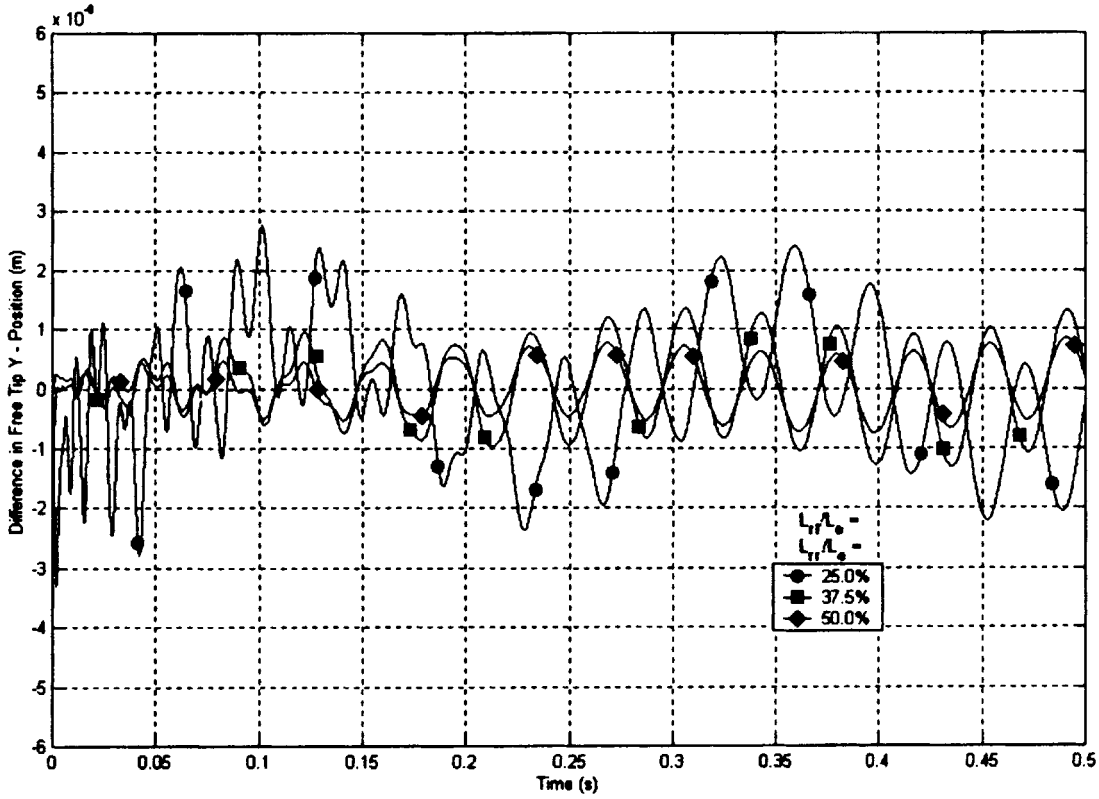

Fig. 11. Effect of rigid part w.r.t element length.

https://doi.org/10.1017/S0263574703005587 Published online by Cambridge University Press

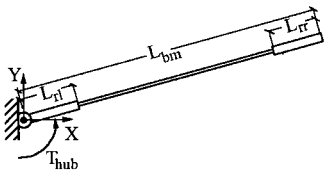

Fig. 12. Rotating flexible beam.

Results of proposed formulation: The obtained results are shown in Figures 16 and 17. The constraint equations for the meshing in this are given as:

$$x_1 = x_0 = 0$$
$$y_1 = y_0 = 0 \qquad (17)$$

It is known that numerical solution of ordinary differential equations is a far simpler and numerically more efficient task than solving nonlinear differential algebraic equations. When employing the proposed formulation for approximating the short rigid zones, the resulting constraint equations are linear equality constraints as in Equation (17). The linear equality constraints can be readily used to reduce the total number of differential equations, while maintaining a set of ordinary differential equations. In case of conventional formulations for the rigid zones, the resulting constraint equations are irreducible nonlinear equations (Equation (16)), which means a differential algebraic solver is necessary (except for trivially simple cases). Thus, the advantage of employing the proposed model is established.

3.3. Example #3: Flexible three-link manipulator

In order to demonstrate the capability of the proposed technique, the motion of a three-link manipulator (Figure 18) moving in a horizontal plane is simulated. Manipulator main data is given in Table II.

To the best of the authors' knowledge, no analytical solution exists for such a problem. Moreover, solutions using conventional finite element or multi-body dynamics techniques will include complicated nonlinear algebraic constraint equations along with the differential equations of motion. This case study presents the solution obtained using only the proposed technique. It is mainly directed to showing that the effect of the rigid (or higher stiffness) zones at the connections between links and joints should not be ignored.

Results of proposed formulation: Each of the manipulator revolute joint actuators rise 45° in a parabolic motion (Figure 19) within 2.8 seconds, then maintain their position. An animated display of the manipulator motion within the first 3 seconds is shown in Figure 20. The motion of the flexible-link manipulator generally follows that of the equivalent rigid-link manipulator while oscillating about it. Figure 21 gives the position of the manipulator end effector.

4. REMARKS AND DISCUSSION

It is observed that increasing the length of the rigid parts with respect to the total beam length has the general effect of increasing the error in the proposed formulation. On the other hand, increasing the ratio of the rigid part to that of the element length decreases the error in the proposed formulation since it significantly increases the stiffness of the element containing the rigid part. On the whole however, the error level in the proposed formulation is low enough for the solution obtained using the proposed formulation to be also considered sufficiently accurate.

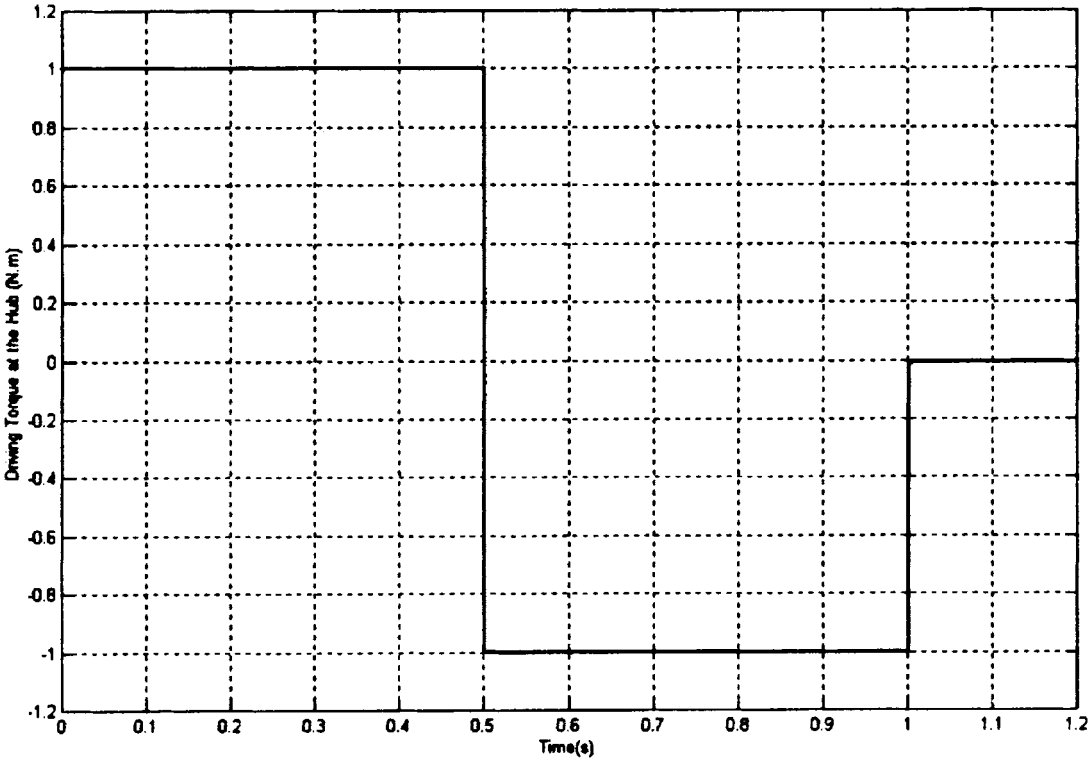

Fig. 13. Driving torque at the hub.

https://doi.org/10.1017/S0263574703005587 Published online by Cambridge University Press

Fig. 14. (a) Orientation at the hub. (b) Orientation at the free tip. (c) X – Position of free tip. (d) Y – Position of free tip.

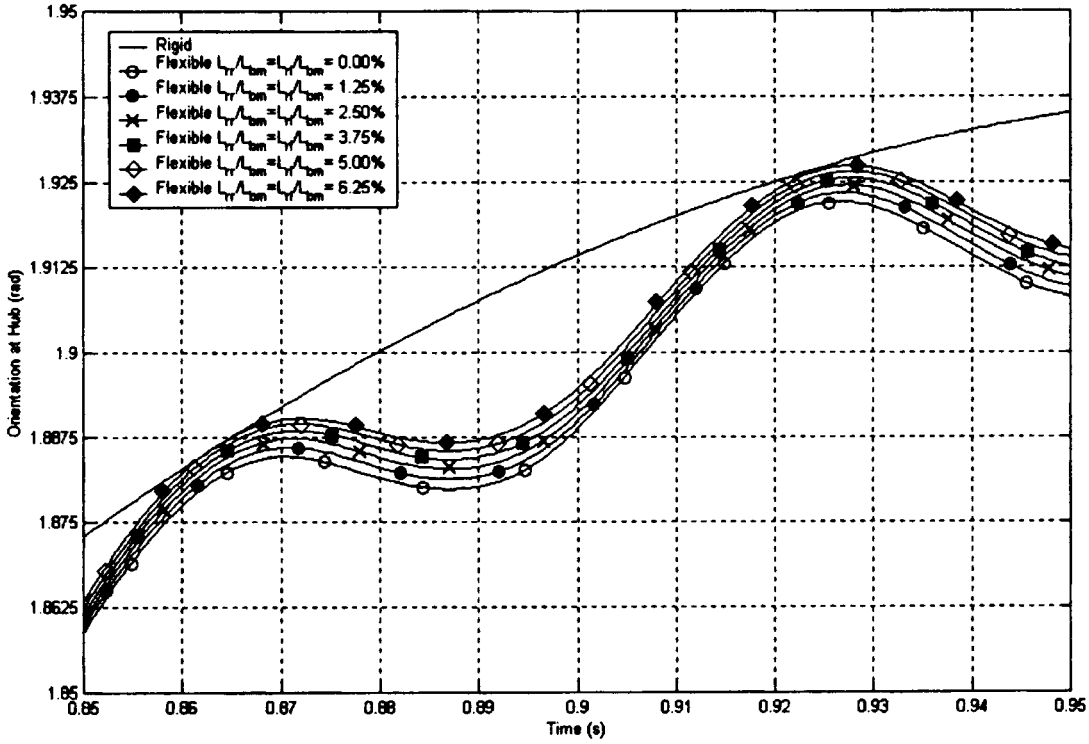

Fig. 15. Response for different rigid part length.

As it may seem, the theoretical limit of the feasibility of using the proposed formulation is that the length of the rigid part must be less than that of the element length. Otherwise, the length of flexible part of the element (Figure 6) will be zero and thus its stiffness would be infinite causing fatal errors for the numerical solver. Practically however, the limitation on the use of the proposed formulation is merely convenience, which in turn, depends on several factors such as the time stepping technique used for the solution of the system differential equations and the speed of the computer used.

Time stepping techniques generally have a minimum time step value if an acceptable solution is to be obtained.[30] The minimum time step value is dependent both on the used technique and the stiffness of system. The higher the stiffness, the smaller the required time step. Table III

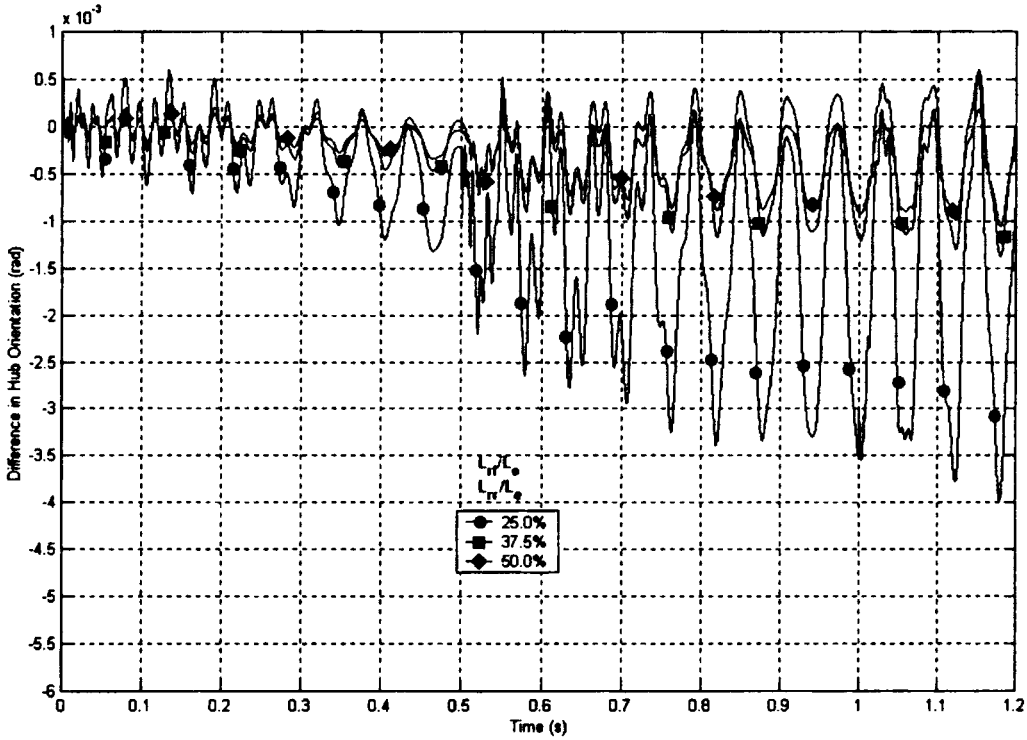

Fig. 16. Effect of rigid part w.r.t element length.

https://doi.org/10.1017/S0263574703005587 Published online by Cambridge University Press

Fig. 17. (a) Orientation at the hub. (b) X – Position of free tip. (c) Y – Position of free tip. (d) Orientation at the free tip.

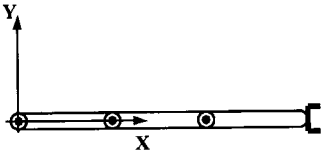

Fig. 18. Case study #3 – three link manipulator.

compares the minimum time step values for different solution conditions of example #1 using the proposed formulation when using fourth order Runge-Kutta for numerical integration of the system differential equations. The minimum time step values in the table were obtained using trial & error, thus they are not very accurate, but they serve only for qualitative comparison. It is observed that at very high rigid part to element length ratio (such as 75%), there is a violent decrease in the minimum time step value, which renders the use of the proposed formulation in such cases impractical.

Also for comparing trends of motion, the response of the no-rigid parts manipulator arm of example #2 is given in Figure 14 when there is no damping, only stiffness associated damping and mass and stiffness associated damping. Although not the main objective of this paper, Figure 14 provides insight to the effect of the different damping forms. Mass associated damping dampens the

Table II. Data of Example #3.

All Links are Identical, No End-Effector Payload	
Link length (L_{bm})	0.8 m
Length of Left Rigid Zone	0.05 m
Length of Right Rigid Zone	0.05 m
Modulus of Elasticity × Cross Sectional Area (E_eA_e	1.8×10 N
Modulus of Elasticity × Second Moment of Area (E_eI_e)	13.5 N . m^2
Mass Associated Damping Constant (α)	0.0
Stiffness Associated Damping Constant (β)	0.0
Mass per unit length	0.72 kg/m
Number of Elements per link	4
Plane of motion	Horizontal Plane
Loading	No loading
Simulation time	6.0 s

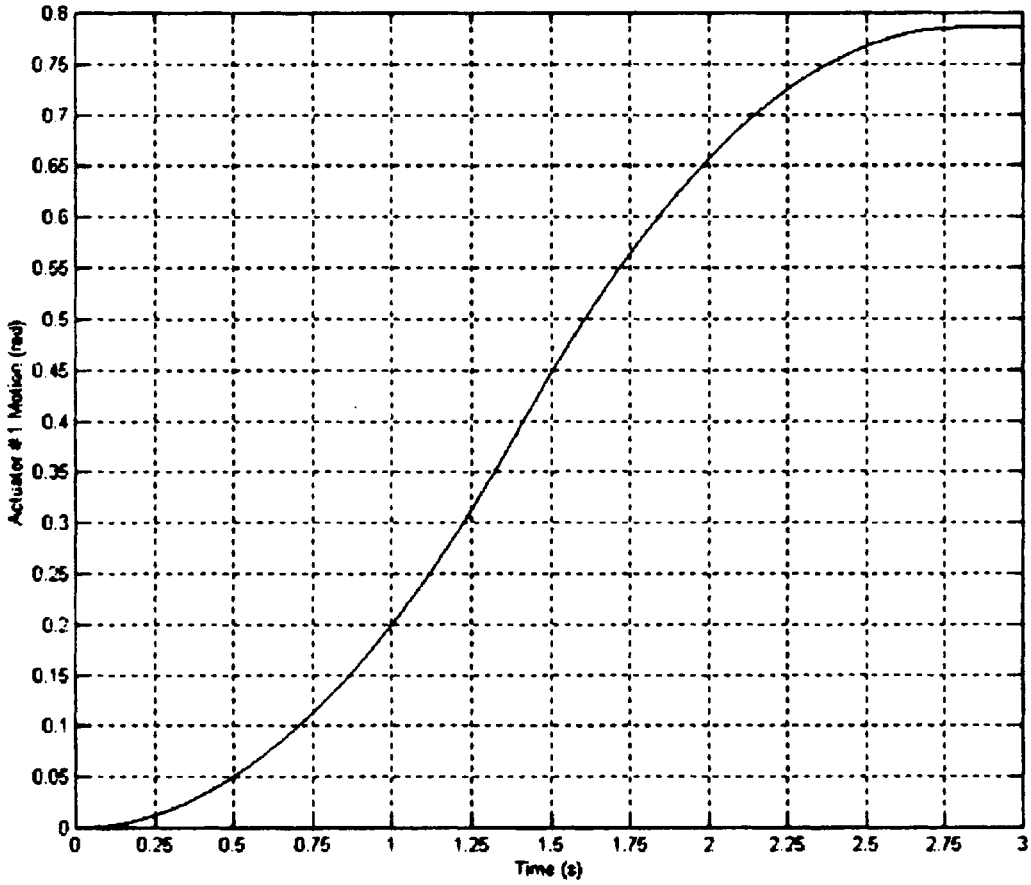

Fig. 19. Case study #3 – actuator's motion.

https://doi.org/10.1017/S0263574703005587 Published online by Cambridge University Press

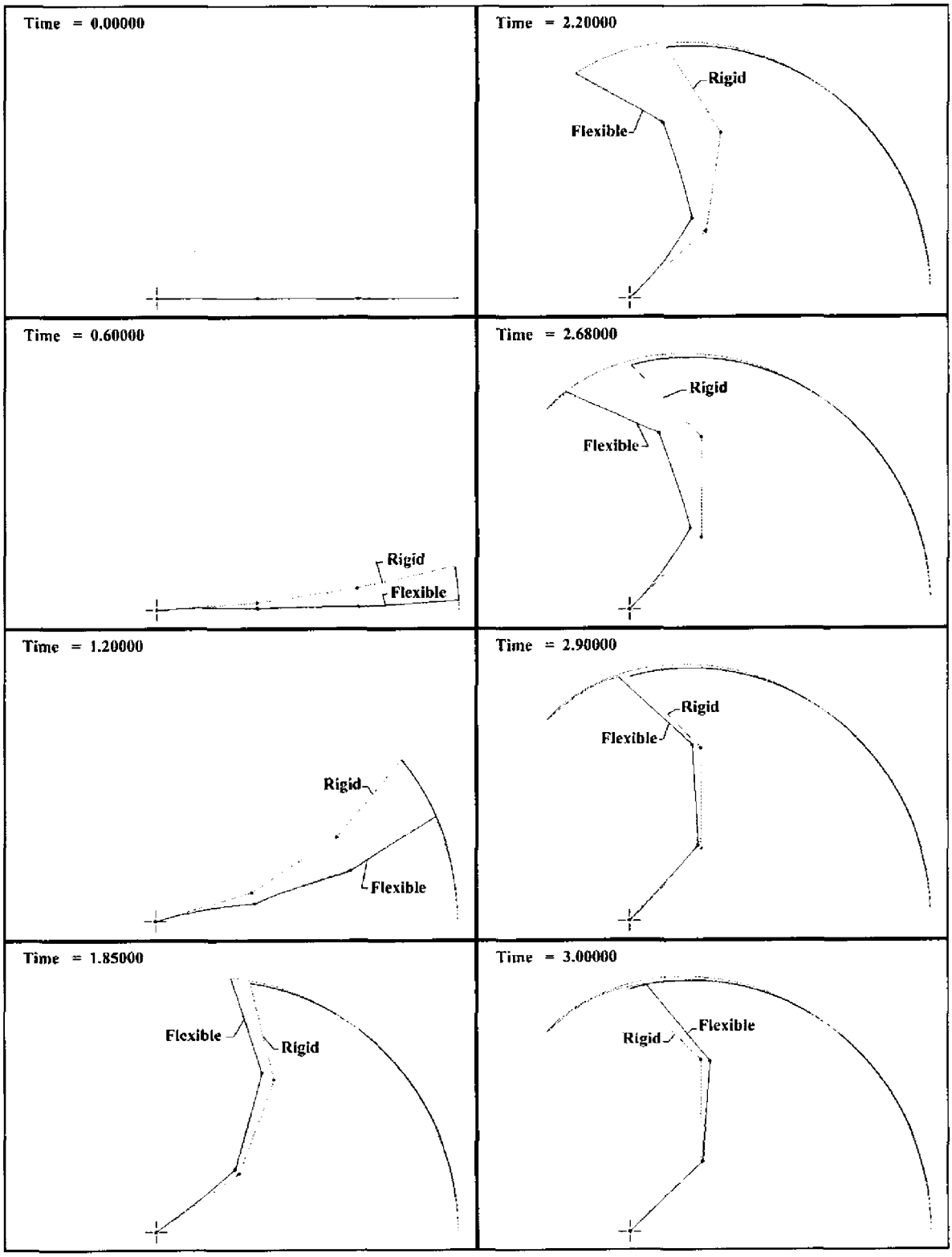

Fig. 20. Case study #3 – animated display.

gross motion of the body, while stiffness associated damping affects most of the high frequency ripples of the flexible body and has no effect on the gross motion.

In case of a multi-link manipulator, the equation reduction necessary for the conventional solution is complicated if it is to be symbolically done, therefore a numerical technique such as that presented in reference [29] would be necessary. On the other hand, the constraint equations for the meshing in proposed formulation are far simpler (Equation (15)) and reduction of the differential equations is straightforward, thus the same time stepping numerical techniques can be applied to a multi-link manipulator.

It is also noticed that the deviation between the flexible-link manipulator and the equivalent rigid-link manipulator is more evident in the cases of multi-link manipulators than in the case of single-link manipulators. Also the deviation

https://doi.org/10.1017/S0263574703005587 Published online by Cambridge University Press

Fig. 21. (a) X – Position of end effector. (b) Y – Position of end effector. (c) Y – Orientation of end effector.

Table III. Minimum Time Step for Problem Solution using Fourth Order Runge-Kutta.

$\frac{L_{rl}}{L_{Bm}}=\frac{L_{rr}}{L_{Bm}}$ (%)	Solution time step (s)			
	4 – Elements per Link	6 – Elements per Link	8 – Elements per Link	12 – Elements per Link
0.00	2.5e-6	1.0e-6	5.5e-7	2.5e-7
1.25	2.5e-6	1.0e-6	5.5e-7	2.5e-7
2.50	2.0e-6	1.0e-6	5.5e-7	2.0e-7
3.75	2.0e-6	9.5e-7	5.0e-7	1.5e-7
5.00	2.0e-6	9.0e-7	4.5e-7	1.5e-7
6.25	2.0e-6	8.5e-7	4.0e-7	4.0e-8

between the simulated motion taking into consideration the effect of rigid zones and the simulation ignoring it is more evident.

Extension of this approach to three dimensional manipulators would be pursued in future work. The main expected challenges would be the selection of rotational coordinates and derivation of the appropriate mass matrix. Extending the rigid-zone approximation to three dimensional analysis is a straight forward task because all stiffness forces are calculated in the local coordinate systems of the elements.

5. CONCLUSIONS

Treatment of link flexibility in the literature often ignores the practical side that rigid or higher stiffness regions exist at the connections to joints. Numerical simulation shows that ignoring the rigid parts at connections may, in some cases, lead to large errors. A proposed flexible multi-body dynamics technique is used to include the effect of the rigid tips in numerical simulation. The proposed technique involves beam elements that can be part rigid and part flexible, which leads to simplification of the constraint equations imposed by the existence of revolute joints. The effectiveness of the proposed technique in simplifying the dynamic equations of the system is demonstrated by two case studies. A third case study is included in order to demonstrate the technique capability in simulating multi-link manipulators. Accuracy of the proposed technique is good over a wide range of system parameter values.The main limitation to using the technique is that the element containing a rigid part must also contain a sufficient flexible portion.

Acknowledgement

This paper is sponsored by the US-Egypt Science and Technology Joint Fund in Cooperation with the American National Science Foundation and Egyptian Ministry of Scientific Research, under Project No. OTH3–004–002.

References

1. R.H. Cannon Jr. and D.E. Rosenthal, "Experiments in Control of Flexible Structures with non-collated Sensors and Actuators", *Journal of Guidance, Control and Dynamics* **7**(5), 546–553 (1984).
2. E. Schmitc, "Dynamics and Control of a Planar Manipulator with Elastic Links", *Proceedings of the 25th Conf. On Decision and Control*, Athens, Greece (1986) pp. 1135–1139.
3. C.M. Oakley and R.H. Cannon Jr., "Dynamics and Control of a Planar Manipulator with Elastic Links", *Proceedings of the American Control Conference*, Piscataway, NJ, USA (1989) pp. 1381–1388.
4. W. Yim, J. Zuang and S.N. Singh, "Experimental Two Axis Vibration Suppression and Control of a Flexible Robot Arm", *Journal of Robotic Systems* **10**(3), 321–343 (1993).
5. G.R. Eisler, R.P. Robinett, D.J. Segalman and J.D. Feddema, "Approximate Optimal Trajectories for Flexible-Link Manipulator Slewing using Recursive Quadratic Programming", *Journal of Dynamic Systems, Measurement and Control* **115**, 405–410 (1993).
6. W. Khalil and F. Boyer, "Efficient Calculation of Computed Torque Control of Flexible Manipulators", *Proceedings of the 1995 IEEE Int. Conf. on Robotics and Automation*, Nagoya, Japan (1995) **Vol.1**, pp. 609–614.
7. E. Shaki, J. Dayan and M. Shoham, "Comparison of Robot Force-Control Methods", *International Journal of Modeling & Simulation* **18**, No. 3, 173–178 (1998).
8. D. Sun and J.K. Mills, "Study on Piezoelectric Actuators in Control of a Single-Link Flexible Manipulator", *Proceedings of the IEEE Conf. on Robotics and Automation*, Detroit, USA (1999) pp. 849–854.
9. C. Chen and Y. Yin, "Fuzzy Logic Control of a Moving Flexible Manipulator", *Proceedings of the 1999 IEEE Int. Conf. on Control Applications and IEEE Int. Symposium on Computer Aided Control System Design*, Kohala Coast, USA (1999) pp. 315–320.
10. F. Bellezza, L. Lanari and G. Ulivi, "Exact Modeling of the Flexible Slewing Link", *Proceedings of the IEEE Conf. on Robotics and Automation*, Cincinnati, OH, USA (1990) pp. 734–739.
11. M. Giovagnoni, "Linear Decoupled Models for a Slewing Beam Undergoing Large Rotations", *Journal of Sound and Vibration* **164**, No. 3, 485–501 (1993).
12. X. Cyril, J. Angeles and A.K. Misra, "Flexible Link Robotic Manipulator Dynamics", *Proceedings of the 1989 American Control Conf.*, Piscataway, USA, June (1989) pp. 2346–2351.
13. R. L. Mayes and R. G. Eisler, "Experimental Characterization of a Flexible Two Link Manipulator Arm", *Proceedings of the 14th Biennial ASME Design Technical Conf. On Mechanical Vibrations and Noise*, Albuquerque, USA, September (1993) pp. 109–113.
14. S.K. Idler, "Open Loop Flexibility Control in Multi-body System Dynamics", *Mechanism and Machine Theory* **30**, No. 6, 861–869 (1995).
15. A.A. Shabana, "Flexible Multi-body Dynamics: Review of Past and Recent Developments", *Multi-body System Dynamics* **1**, 189–222 (1997).
16. A.A. Shabana, *Dynamics Multi-body Systems* (Cambridge University Press, Cambridge, UK, 1998).
17. A.A. Shabana and R. Schwertassek, "Equivalence of the Floating Frame of Reference Approach and Finite Element Formulations", *Int. J. of Nonlinear Mechanics* **33**, No. 3, 417–432 (1998).

18. A.A. Shabana, "An Absolute Nodal Coordinate Formulation for Large Rotation and Deformation Analysis of Flexible Bodies", *Technical Report No. MB96-UIC* (Department of Mechanical Engineering, University of Illinois at Chicago, March 1996).
19. J.D. Cornnelly and R.L. Huston, "The Dynamics of Flexible Multi-body Systems: A Finite Segment Approach", *Computers and Structures* **50**, No. 2, 255–261 (1994).
20. S.M. Megahed and K.T. Hamza, "A Systematic Algorithm for Flexible Manipulators Simulation", *Proceedings of Cairo University 7th Mechanical Design and Production Conference*, Cairo, Egypt (February, 2000) pp. 27–36.
21. S.M. Megahed and K.T. Hamza, "Modeling of Planar Flexible Link Manipulators: Parameter Identification using Genetic Algorithm", *Proceedings of the ASME 26th Biennial Mechanisms and Robotics Conference DETC 2000/MECH-14184*, Baltimore, Maryland, September (2000) (on CD).
22. K.T. Hamza, "Modeling,, Simulation and Control of Robotic Manipulators with Flexible Links", *Masters Thesis* (Mechanical Design and Production Department, Cairo University, June 2001).
23. S.M. Megahed, *Principles of Robot Modeling and Simulation* (John Wiley & Sons Ltd., 1993).
24. W.H. Press, S.A. Teukolsky, W.T. Vetterling and B.P. Flannery, *Numerical Recipes in Fortran*, Second Edition (Cambridge University Press, New York, 1992).
25. G.N. Sandor and A.G. Erdman, *Advanced Mechanism Design: Analysis and Synthesis* (Prentice-Hall Inc., Engelwood Cliffs, New Jersey, USA, 1984).
26. C.E. Knight, *The Finite Element Method in Mechanical Design* (PWS-KENT Publishing Co., Boston, USA 1993).
27. C.T. Sun and Y.P. Lu, *Vibration Damping of Structural Elements* (Prentice Hall PTR, Engelwood Cliffs, New Jersey, USA, 1995).
28. W.T. Thomson, *Theory of Vibration with Applications*, Fourth Edition (Chapman & Hall, London, UK, 1993).
29. A.A. Shabana, *Computational Dynamics* (John Wiley & Sons Ltd., 1994).
30. C.W. Bert and J.D. Stricklin, "Comparative Evaluation of Six Different Numerical Integration Methods for Non-Linear Dynamic Systems", *Journal of Sound and Vibration* **127**, No. 2, 221–229 (1988).

https://doi.org/10.1017/S0263574703005587 Published online by Cambridge University Press